



# Synthesis, characterization and reactivity of the $\omega$ -haloalkyl complexes [[ $(\eta^5\text{-C}_5\text{R}_5)\text{W}(\text{CO})_3\{(\text{CH}_2)_n\text{X}\}$ ] ( $\text{R} = \text{H}$ , $n = 3\text{--}7$ , $\text{X} = \text{Br}$ and $\text{I}$ ; $\text{R} = \text{CH}_3$ , $n = 3, 4$ , $\text{X} = \text{Br}$ and $\text{I}$ )

Xiaolong Yin \*, John R. Moss <sup>1</sup>

Department of Chemistry, University of Cape Town, Rondebosch 7700, South Africa

Received 21 April 1998; received in revised form 12 June 1998

## Abstract

The new  $\omega$ -bromoalkyl tungsten complexes  $[\text{CpW}(\text{CO})_3\{(\text{CH}_2)_n\text{Br}\}]$  ( $n = 5\text{--}7$ ) and  $[\text{Cp}^*\text{W}(\text{CO})_3\{(\text{CH}_2)_n\text{Br}\}]$  ( $n = 4$ ) were prepared in good yields by the reactions of  $\text{Na}[\text{CpW}(\text{CO})_3]$  or  $\text{Na}[\text{Cp}^*\text{W}(\text{CO})_3]$  with the appropriate dibromoalkanes. The iodoalkyl complexes  $[\text{CpW}(\text{CO})_3\{(\text{CH}_2)_n\text{I}\}]$  ( $n = 3\text{--}7$ ) and  $[\text{Cp}^*\text{W}(\text{CO})_3\{(\text{CH}_2)_n\text{I}\}]$  ( $n = 3$  and  $4$ ) were prepared by reacting  $[\text{CpW}(\text{CO})_3\{(\text{CH}_2)_n\text{Br}\}]$  or  $[\text{Cp}^*\text{W}(\text{CO})_3\{(\text{CH}_2)_n\text{Br}\}]$  with sodium iodide, or by reacting the  $\text{Na}[\text{CpW}(\text{CO})_3]$  with the appropriate diiodoalkanes. These new complexes have been fully characterized by elemental analyses, IR,  $^1\text{H}$ -,  $^{13}\text{C}$ -NMR and mass spectroscopy. The thermal and electrochemical properties of some of the haloalkyl complexes are reported. The reaction of  $[\text{CpW}(\text{CO})_3\{(\text{CH}_2)_3\text{Br}\}]$  with 3,5-dihydroxybenzyl alcohol gave both the mono- and the di-tungsten benzyl alcohol complexes  $[\{\text{CpW}(\text{CO})_3(\text{CH}_2)_3\text{O}\}\{\text{C}_6\text{H}_3(\text{OH})\text{-CH}_2\text{OH}]$  and  $[\{\text{CpW}(\text{CO})_3(\text{CH}_2)_3\text{O}\}_2(\text{C}_6\text{H}_3)\text{-CH}_2\text{OH}]$ . The later complex reacted with  $\text{CBr}_4$  and  $\text{PPh}_3$  to give the benzyl bromide complex  $[\{\text{CpW}(\text{CO})_3(\text{CH}_2)_3\text{O}\}_2(\text{C}_6\text{H}_3)\text{-CH}_2\text{Br}]$ . The reaction of  $[\text{CpW}(\text{CO})_3\{(\text{CH}_2)_3\text{Br}\}]$  with 1,1,1-tris(4'-hydroxyphenyl)ethane gave the tri-nuclear tungsten complex  $[\{\text{CpW}(\text{CO})_3(\text{CH}_2)_3\text{O}\}(\text{C}_6\text{H}_4)_3\text{-CCH}_3]$ . © 1999 Published by Elsevier Science S.A. All rights reserved.

**Keywords:** Haloalkyl; Tungsten; Cyclopentadienyl; Carbonyl; Bromide; Iodide

## 1. Introduction

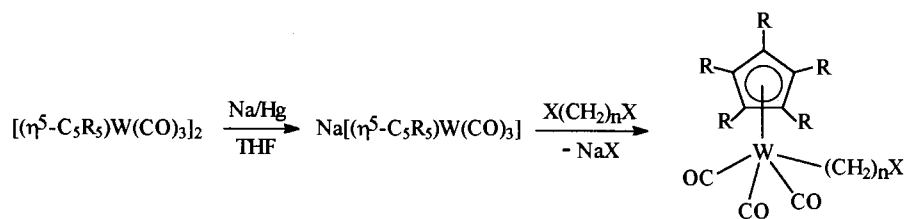
Haloalkyl transition metal complexes of the type  $[\text{LyM}\{(\text{CH}_2)_n\text{X}\}]$  ( $\text{Ly} = \text{ligands}$ ,  $\text{M} = \text{transition metal}$ ,  $\text{X} = \text{halogen}$ ,  $n \geq 1$ ), which were quite rare 30 years ago [1], are now well known [2–10]. The synthesis and chemistry of some haloalkyl complexes have recently been extensively investigated [3–10] and comprehensively reviewed by Moss and Friedrich [2,11]. The haloalkyl complexes show interesting and novel chemistry and can be used, for example, as precursors for a

wide range of useful compounds including acyclic and cyclic carbene complexes [12–14], homo- and hetero-bimetallic hydrocarbon-bridged complexes [13,15–17], dendrimers [18,19], as well as many other classes of functionalized alkyl compounds [9].

The complexes  $[(\eta^5\text{-C}_5\text{R}_5)\text{W}(\text{CO})_3\{(\text{CH}_2)_n\text{X}\}]$  (where  $n = 1$ ;  $\text{R} = \text{H}$  and  $\text{CH}_3$ ,  $\text{X} = \text{Cl}$ ,  $\text{Br}$  and  $\text{I}$ ) have been reported [8,9]. Although the complexes  $[(\eta^5\text{-C}_5\text{R}_5)\text{W}(\text{CO})_3\{(\text{CH}_2)_n\text{X}\}]$  ( $\text{X} = \text{Br}$ ;  $\text{R} = \text{H}$ ,  $n = 3$  and  $4$  [1];  $\text{R} = \text{CH}_3$ ,  $n = 3$  [14]) have been reported by King and co-workers in 1967, the reactivity of these complexes has been less studied [1,2,12–14]. The reaction of  $\text{Na}[\text{CpW}(\text{CO})_3]$  with 1, $n$ -diiodoalkanes ( $n = 3, 4$ ) was reported [13] to yield the hydrocarbon-bridged complexes  $[\text{Cp}(\text{CO})_3\text{W}(\text{CH}_2)_n\text{W}(\text{CO})_3\text{Cp}]$  ( $n = 3, 4$ ), and the iodoalkyl complexes  $[\text{CpW}(\text{CO})_3\{(\text{CH}_2)_n\text{I}\}]$  ( $n = 3$  and  $4$ ) were suggested as intermediates in these reactions

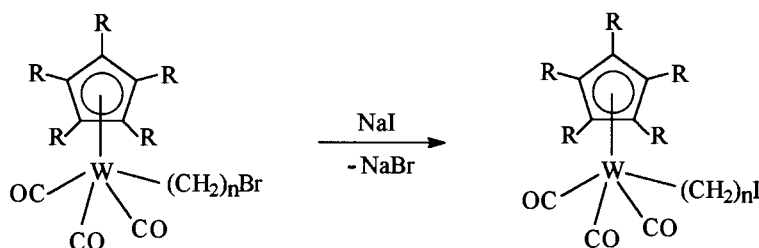
\* Corresponding author. Current address: Department of Chemistry, University of Louisville, Louisville, KY 40292, USA. Tel.: +1 502 8527840; fax: +1 502 8528149; e-mail: x0yin001@homer.louisville.edu

<sup>1</sup> Fax: +27 21 6897499; e-mail: jrm@psipsy.uct.ac.za.



R	X	n	Compd. no
H	Br	3	1
H	Br	4	2
H	Br	5	3
H	Br	6	4
H	Br	7	5
H	I	4	7
CH <sub>3</sub>	Br	3	11
CH <sub>3</sub>	Br	4	12

Scheme 1.



R	n	Compd. no
H	3	6
H	5	8
H	6	9
H	7	10
CH <sub>3</sub>	3	13
CH <sub>3</sub>	4	14

Scheme 2.

[13]. The intermediates could also be isolated under suitable conditions as was demonstrated by Scott [20], who successfully isolated  $[\text{CpW}(\text{CO})_3\{(\text{CH}_2)_n\text{I}\}]$  ( $n = 4$  and 5) but with only partial characterization. Here we report the synthesis and full characterization of an extensive series of haloalkyl complexes  $[(\eta^5\text{-C}_5\text{R}_5\text{W}(\text{CO})_3\{(\text{CH}_2)_n\text{X}\})]$  ( $\text{R} = \text{H}$ ,  $n = 3\text{--}7$ ,  $\text{X} = \text{Br}$ ,  $\text{I}$ ;  $\text{R} = \text{CH}_3$ ,  $n = 3, 4$ ,  $\text{X} = \text{Br}$  and  $\text{I}$ ). Furthermore, the reactivity of these complexes leading to some bi- and polynuclear complexes is also reported.

## 2. Results and discussions

### 2.1. Synthesis of $[(\eta^5\text{-C}_5\text{R}_5\text{W}(\text{CO})_3\{(\text{CH}_2)_n\text{X}\})]$

The bromoalkyl complexes  $[(\eta^5\text{-C}_5\text{R}_5\text{W}(\text{CO})_3\{(\text{CH}_2)_n\text{Br}\})]$  ( $\text{R} = \text{H}$ ,  $n = 3$ , **1**; 4, **2**; 5, **3**; 6, **4**; 7, **5**;

$\text{R} = \text{CH}_3$ ,  $n = 3$ , **11**, **4**, **12**) have been prepared in good yields by the reaction of  $\text{Na}[(\eta^5\text{-C}_5\text{R}_5\text{W}(\text{CO})_3)]$  with an excess 1, $n$ -dibromoalkanes in THF as shown in Scheme 1. This method is similar to that reported by King and co-workers [1] for the preparation of **1** and **2** in low yields. Bailey and co-workers [14] have also applied this method to prepare **11**.

The reactions were monitored by IR spectroscopy, and stopped after all the  $\text{Na}[(\eta^5\text{-C}_5\text{R}_5\text{W}(\text{CO})_3)]$  was consumed. It is found that the reaction of  $\text{Na}[\text{CpW}(\text{CO})_3]$  with 1, $n$ -dibromoalkanes at r.t. is chain-length dependent. Thus, the longer the polymethylene chain, the longer the reaction time required. Complexes **4** and **5** could only be prepared by refluxing the reaction mixture overnight. The relatively slow reaction rate of  $\text{Na}[\text{CpW}(\text{CO})_3]$  with 1, $n$ -dibromoalkanes, compared with that of  $\text{Na}[\text{CpFe}(\text{CO})_2]$ , is due to the weak nucleophilicity of the tungsten anion [21]. The

Table 1  
Data for  $[\text{Cp}^*\text{W}(\text{CO})_3\{(\text{CH}_2)_n\text{X}\}]$

Compound number	X	n	Yield (%)	M.p. (°C)	IR $\nu(\text{CO})^a$ ( $\text{cm}^{-1}$ )	Elemental analysis (%)	
						C: found (calc.)	H: found (calc.)
1 <sup>b</sup>	Br	3	66	108–110	2020s, 1929vs	29.30(29.00)	2.42(2.40)
2 <sup>c</sup>	Br	4	45	58–66	2017s, 1927vs	31.12(30.70)	2.75(2.77)
3	Br	5	50	122–125	2017s, 1927vs	32.35(32.33)	3.06(3.13)
4	Br	6	49	61–63	2017s, 1927vs	34.08(33.83)	3.47(3.45)
5	Br	7	37	44–48	2017s, 1927vs	35.73(35.25)	3.79(3.75)
6	I	3	70	81–84	2020s, 1929vs	26.92(26.32)	2.21(2.21)
7 <sup>d</sup>	I	4	56	67–69	2018s, 1927vs	28.11(27.91)	2.45(2.51)
8 <sup>e</sup>	I	5	63	127–130	2017s, 1927vs	29.97(29.46)	2.65(2.85)
9	I	6	62	57–58	2017s, 1927vs	31.46(30.91)	3.14(3.15)
10	I	7	57	49–51	2016s, 1927vs	32.57(32.28)	3.44(3.43)

<sup>a</sup> IR in hexane.

<sup>b</sup> Ref. [1], m.p. 109–112°C.

<sup>c</sup> Ref. [1], m.p. 66–68°C, DSC studies showed that this complex might exist in different crystal forms (see Section 2).

<sup>d</sup> Ref. [20], m.p. 69–71°C.

<sup>e</sup> Ref. [20], m.p. 129–131°C.

$\text{Na}[\text{Cp}^*\text{W}(\text{CO})_3]$  is found to be more reactive than the Cp analogs due to the increased nucleophilicity caused by the Cp\* ligand. It is also found, as expected, that the reaction of  $\text{Na}[\text{Cp}^*\text{W}(\text{CO})_3]$  with 1,4-diiodobutane, to give the complex **7**, is faster than its reaction with 1,4-dibromobutane.

Complexes **1–5**, **7**, **11** and **12** were obtained in good yields as yellow crystalline solids after purification by chromatography and recrystallization. They are moderately air stable, both in solution and in the solid state for short periods of time.

The iodoalkyl complexes  $[(\eta^5\text{-C}_5\text{R}_5)\text{W}(\text{CO})_3\{(\text{CH}_2)_n\text{I}\}]$  (R = H, **6**; 5, **8**; 6, **9**; 7, **10**; R = CH<sub>3</sub>, **13**, **4**, **14**) have been successfully prepared in high yields by the reaction of the corresponding bromoalkyl complexes with NaI in acetone at r.t. for 1–2 days, as shown in Scheme 2. Complexes **7** and **8** were previously prepared in this laboratory via a similar route, but were not fully characterized [20].

The preparation of **6** and **13**, from the reaction of **1** and **11** with NaI, respectively, is in contrast to reports [12,14] that reaction of **1** and **11** with LiI in refluxing 1,2-dimethoxyethane or THF, respectively, gave the

*trans*-2-oxacyclopentylidene tungsten complexes as shown below:



The different products obtained from the reactions of **1** and **11** with NaI under the above reaction conditions may thus be due to the reaction temperature.

The method, shown in Scheme 2, has been previously used to convert bromoalkyl complexes of iron and ruthenium to the corresponding iodoalkyl complexes [5,6].

The iodoalkyl complexes, like the bromoalkyl complexes, are yellow crystalline solids. They have similar melting points to the corresponding bromoalkyl complexes, except **6**, which has a much lower melting point than **1**. The iodoalkyl complexes are more sensitive to light and air than their bromoalkyl analogs.

## 2.2. Characterization of $[(\eta^5\text{-C}_5\text{R}_5)\text{W}(\text{CO})_3\{(\text{CH}_2)_n\text{X}\}]$

The haloalkyl complexes (**1–14**) have been fully characterized. The yields, melting points and IR spectra, as well as elemental analysis data for the haloalkyl com-

Table 2  
Data for  $[\text{Cp}^*\text{W}(\text{CO})_3\{(\text{CH}_2)_n\text{X}\}]$

Compound number	X	n	Yield (%)	M.p. (°C)	IR $\nu(\text{CO})^a$ ( $\text{cm}^{-1}$ )	Elemental analysis (%)	
						C: found (calc.)	H: found (calc.)
11 <sup>b</sup>	Br	3	68	83–85	2007s, 1914vs	36.93(36.60)	4.05(4.03)
12	Br	4	62	53–55	2005s, 1913vs	38.09(37.87)	4.33(4.30)
13	I	3	78	83–85	2006s, 1914vs	34.26(33.59)	3.76(3.70)
14	I	4	71	63–65	2005s, 1913vs	35.30(34.84)	4.00(3.96)

<sup>a</sup> IR in hexane.

<sup>b</sup> Ref. [14], m.p. 80–82°C.

Table 3  
<sup>1</sup>H-NMR data for [CpW(CO)<sub>3</sub>{(CH<sub>2</sub>)<sub>n</sub>X}] (400 MHz, CDCl<sub>3</sub>)<sup>a</sup>

Compound	number	X	n	Cp	CH <sub>2</sub> X <sup>3</sup> J/(HH)	CH <sub>2</sub> CH <sub>2</sub> X <sup>3</sup> J/(HH)	α-CH <sub>2</sub>	β-CH <sub>2</sub>	γ-CH <sub>2</sub> <sup>3</sup> J/(HH)	δ-CH <sub>2</sub> <sup>3</sup> J/(HH)	ε-CH <sub>2</sub>
1	3	Br	5.41, 5H, s	3.33, 2H, t, 7.2	2.06, 2H, qn, 7.2	1.49, 2H, m					
2	4	Br	5.41, 5H, s	3.45, 2H, t, 7.2	1.87, 2H, qn, 7.2	1.50, 2H, m	1.67, 2H, m				
3	5	Br	5.37, 5H, s	3.40, 2H, t, 6.7	1.88, 2H, qn, 6.9	1.54, 4H, m		1.43, 2H, m			
4	6	Br	5.37, 5H, s	3.40, 2H, t, 6.8	1.84, 2H, qn, 7.2	1.55, 4H, m		1.42, 2H, m	1.32, 2H, qn, 7.2		
5	7	Br	5.37, 5H, s	3.40, 2H, t, 7.2	1.85, 2H, qn, 7.2	1.54, 4H, m		1.41, 2H, m	1.32, 4H, m		
6	3	I	5.39, 5H, s	3.11, 2H, t, 7.2	2.02, 2H, d-qn, 7.6	1.47, 2H, d-t	1.65, 2H, m				
7	4	I	5.40, 5H, s	3.22, 2H, t, 7.2	1.83, 2H, qn, 6.8	1.48, 2H, m			1.39, 2H, qn, 7.6		
8	5	I	5.37, 5H, s	3.17, 2H, t, 7.2	1.83, 2H, qn, 7.2	1.52, 4H, m			1.40, 2H, qn, 7.2		
9	6	I	5.37, 5H, s	3.18, 2H, t, 7.2	1.81, 2H, qn, 7.2	1.54, 4H, m			1.31, 2H, m		
10	7	I	5.37, 5H, s	3.19, 2H, t, 7.2	1.82, 2H, qn, 7.2	1.53, 4H, m			1.35, 2H, m		

<sup>a</sup> Coupling constants are given in Hz; α-CH<sub>2</sub> refers to the protons on the CH<sub>2</sub> α to tungsten, etc.

Table 4  
 $^1\text{H-NMR}$  data for  $[\text{Cp}^*\text{W}(\text{CO})_3\{(\text{CH}_2)_n\text{X}\}]$  (400 MHz,  $\text{CDCl}_3$ )<sup>a</sup>

Compound number	X	n	$\text{C}_5(\text{CH}_3)_5$	$\text{CH}_2\text{X}$ $^3J(\text{HH})$	$\text{CH}_2\text{CH}_2\text{X}$ $^3J(\text{HH})$	$\alpha\text{-CH}_2$	$\beta\text{-CH}_2$
<b>11</b> <sup>b</sup>	Br	3	1.97, 15H, s	3.35, 2H, t, 7.2	2.07, 2H, m	0.75, 2H, m	
<b>12</b>	Br	4	1.97, 15H, s	3.42, 2H, t, 7.2	1.91, 2H, qn, 7.2	0.79, 2H, m	1.70, 2H, m
<b>13</b>	I	3	1.98, 15H, s	3.16, 2H, t, 7.2	2.04, 2H, m	0.76, 2H, m	
<b>14</b>	I	4	1.96, 15H, s	3.19, 2H, t, 7.2	1.89, 2H, qn, 7.2	0.78, 2H, m	1.66, 2H, m

<sup>a</sup> Coupling constants are given in Hz,  $\alpha\text{-CH}_2$  refers to the protons on the  $\text{CH}_2$   $\alpha$  to tungsten, etc.

<sup>b</sup> These data are in good agreement with literature values [14].

plexes (**1–14**) are summarized in Tables 1 and 2. All the complexes have been characterized by satisfactory C and H analyses. The  $^1\text{H}$ - and  $^{13}\text{C}$ -NMR, as well as mass spectral data are summarized in Tables 3–8.

### 2.2.1. IR spectroscopy

As seen in Tables 1 and 2, the IR spectra of complexes **1–14** are in good agreement with the data reported for some known compounds [1,14,20]. There is no significant change in the positions of the carbonyl bands in the IR spectra between the bromoalkyl and corresponding iodoalkyl complexes, and there is only a very slight trend towards lower wavenumbers as the carbon chain lengthens from  $n = 3$  to  $n = 5$ . The IR spectra of the Cp complexes are also very similar to those of the long chain alkyl complexes  $[\text{Cp-W}(\text{CO})_3(\text{CH}_2)_n\text{CH}_3]$  ( $n = 5–9$ ) [22]. The  $\nu(\text{CO})$  for the Cp\* complexes is lower than that for the analogous Cp complexes by ca.  $13\text{ cm}^{-1}$ . This is consistent with the increase in electron density on the metal (caused by the Cp\* group), which results in increased back-bonding to the carbonyl groups, and hence, a lower  $\nu(\text{CO})$  [5].

### 2.2.2. $^1\text{H-NMR}$ spectroscopy

The  $^1\text{H-NMR}$  data for complexes **1–14** are summarized in Tables 3 and 4. The  $^1\text{H-NMR}$  data for **11** have been reported by Bailey et al. [14] and our results for the same compound agree well with the reported data. The complexes **1**, **2**, **7** and **8** have also been previously characterized by  $^1\text{H-NMR}$  [1,20]. From Tables 3 and 4,

it can be seen that the  $\alpha\text{-CH}_2$  ( $\alpha$  to tungsten) resonances appear at ca. 1.5 ppm for the Cp complexes and at ca. 0.8 ppm for the Cp\* complexes. No coupling between tungsten and the  $\alpha\text{-CH}_2$  protons is observed. The observation that the  $\alpha\text{-CH}_2$  protons of the Cp\* complexes are more shielded than those of the Cp analogs may be due to the increased electron density at the tungsten center in these Cp\* complexes. The  $\text{CH}_2\text{X}$  ( $\text{X} = \text{Br}, \text{I}$ ) protons for complexes with  $n = 3$  are also found slightly more shielded than the  $\text{CH}_2\text{X}$  protons for complexes with  $n > 4$ . However, the  $\text{CH}_2\text{X}$  and  $\text{CH}_2\text{CH}_2\text{X}$  protons show no further shift on increasing the chain length beyond  $n = 5$ , suggesting that the effect of the tungsten group on the chain end is now no longer detectable in these complexes. Similar trends were also observed in the haloalkyl iron complexes [5]. The up-field shift of 0.2–0.3 ppm of the  $\text{CH}_2\text{X}$  resonances, as X changes from Br to I, is as expected because of the difference in their electronegativities, however, the effect of the halogen diminishes quickly along the carbon chain.

### 2.2.3. $^{13}\text{C-NMR}$ spectroscopy

No  $^{13}\text{C-NMR}$  data have previously been reported for complexes **1–14** [1,13,20]. The data for complexes **1–14** are given in Tables 5 and 6. Assignments were made by comparison with the  $^{13}\text{C-NMR}$  data reported for the haloalkyl complexes  $[\text{CpFe}(\text{CO})_2\{(\text{CH}_2)_n\text{X}\}]$  ( $n = 3–7$ ,  $\text{X} = \text{Br}, \text{I}$ ) [5] and  $[\text{CpW}(\text{CO})_3\text{R}]$  ( $\text{R} =$  various alkyl groups) [22], as well as by HETCOR experiments.

Table 5  
 $^{13}\text{C-NMR}$  chemical shift data ( $\delta$  ppm) for  $[\text{CpW}(\text{CO})_3\{(\text{CH}_2)_n\text{X}\}]$  (100 MHz,  $\text{CDCl}_3$ )

Compound number	X	n	CO	Cp	$\text{CH}_2\text{X}$	$\text{CH}_2\text{CH}_2\text{X}$	$\alpha\text{-CH}_2$ <sup>a</sup>	$\beta\text{-CH}_2$	$\gamma\text{-CH}_2$	$\delta\text{-CH}_2$	$\varepsilon\text{-CH}_2$
<b>1</b>	Br	3	228.17, 217.36	91.53	37.77	40.09	–14.66				
<b>2</b>	Br	4	228.53, 217.47	91.47	33.49	35.05	–12.44	38.35			
<b>3</b>	Br	5	228.62, 217.60	91.47	32.28	34.11	–10.91	35.88	34.29		
<b>4</b>	Br	6	228.83, 217.57	91.47	32.88	34.09	–10.46	36.62	34.98	27.66	
<b>5</b>	Br	7	228.90, 217.55	91.46	32.84	34.06	–10.21	36.72	35.65	28.20	28.18
<b>6</b>	I	3	228.15, 217.38	91.49	11.70	41.00	–11.92				
<b>7</b>	I	4	228.52, 217.47	91.47	6.99	37.49	–12.61	39.03			
<b>8</b>	I	5	228.68, 217.59	91.47	7.40	33.02	–10.91	36.64	35.66		
<b>9</b>	I	6	228.86, 217.57	91.46	7.36	33.60	–10.45	36.61	34.76	29.99	
<b>10</b>	I	7	228.91, 217.55	91.47	7.37	33.58	–10.21	36.73	35.62	30.50	27.99

<sup>a</sup>  $\alpha\text{-CH}_2$  refers to the  $\text{CH}_2$  carbon  $\alpha$  to tungsten, etc.

Table 6  
 $^{13}\text{C}$ -NMR chemical shift data ( $\delta$  ppm) for  $[\text{Cp}^*\text{W}(\text{CO})_3\{(\text{CH}_2)_n\text{X}\}]$  (100 MHz,  $\text{CDCl}_3$ )

Compound number	X	n	CO	$\text{C}_5(\text{CH}_3)_5$	$\text{CH}_2\text{X}$	$\text{CH}_2\text{CH}_2\text{X}$	$\alpha\text{-CH}_2^a$	$\beta\text{-CH}_2$	$\text{C}_5(\text{CH}_3)_5$
11	Br	3	232.01, 223.01	102.89	38.92	39.88	-3.41		10.36
12	Br	4	232.29, 223.10	102.77	33.49	35.10	-1.02	39.82	10.36
13	I	3	231.97, 223.03	102.91	13.47	40.74	-0.46		10.37
14	I	4	232.30, 223.07	102.77	6.63	37.48	-1.25	40.64	10.36

<sup>a</sup>  $\alpha\text{-CH}_2$  refers to the  $\text{CH}_2$  carbon  $\alpha$  to tungsten, etc.

The chain length or the nature of the halogen have no significant effect on the positions of the CO peaks. Similarly, the chain length and the halogen do not appear to affect the position of Cp or Cp\* peaks very much, although for complexes with  $n = 3$ , the CO peaks are found at a slightly higher field and the Cp or Cp\* peaks at a slightly lower field, compared with those for complexes with  $n > 3$ . The methylene  $\alpha\text{-CH}_2$  carbons in the Cp\* complexes are significantly (ca. 10 ppm) more deshielded than those in the corresponding Cp complexes. So too are the carbonyl carbon peaks, though to a lesser degree (ca. 4 ppm). The deshielding effect is no longer apparent for the  $\beta$ -carbons of the methylene chain.

The effect of the halogen on the  $\delta$  value of the  $\alpha\text{-CH}_2$  carbon, for the complexes where  $n = 3$  and  $n = 4$ , is very apparent, and diminishes gradually with increasing  $n$  from 5 to 7. The peak due to the  $\alpha$ -carbon is shifted up-field for those complexes with smaller values of  $n$ . This is in contrast to what one would expect considering the inductive effect of the halogens. For both the Cp and the Cp\* complexes, the complexes with  $n = 3$  are of particular interest, as the peak for the  $\alpha$ -carbon is at a much higher field for  $\text{X} = \text{Br}$  than for  $\text{X} = \text{I}$ . These observations could possibly be explained in terms of a weak interaction between the halogen and tungsten, as has been suggested for the iron complexes  $[\text{CpFe}(\text{CO})_2\{(\text{CH}_2)_n\text{X}\}]$  [5]. The interaction between tungsten and halogen is also shown by the ca. 4 ppm down-field shift of the peaks of the  $\text{CH}_2\text{X}$  carbon for  $n = 3$ , relative to the corresponding peaks for compounds with  $n = 4\text{--}7$ . Thus as  $n$  increases, the distance between X and tungsten increases, and the effect of their interaction would decrease. Also apparent from the  $^{13}\text{C}$ -NMR data is the large chemical shift difference (ca. 25 ppm) between the  $\text{CH}_2\text{X}$  carbons ( $\text{X} = \text{Br}$  and I), reflecting the different electron withdrawing abilities of the halogens.

#### 2.2.4. Mass spectra

Low resolution electron impact mass spectra were obtained for all the compounds under discussion. The intensities of the major peaks of  $[\text{CpW}(\text{CO})_3\{(\text{CH}_2)_n\text{X}\}]$  (**1–10**) are reported in Table 7, while those of  $[\text{Cp}^*\text{W}(\text{CO})_3\{(\text{CH}_2)_n\text{X}\}]$  (**11–14**) are reported in Table

8, with probable assignments. The assignment of peaks in the mass spectra of these haloalkyl complexes is complicated by the extensive isotope patterns of tungsten- and bromine-containing ions, which makes the assignment potentially ambiguous.

Molecular ion peaks are observed in the spectra of all the Cp complexes **1–10**, but are of low intensity. Molecular ions are also observed in the spectra of all the Cp\* complexes **11–14** and are of the strongest intensities except in the spectrum of **13**. This difference is largely due to the enhanced stability for these Cp\* complexes. For the Cp complexes, all spectra show weak peaks corresponding to loss of CO from the parent ions, except **2**, **7** and **9**. All spectra also exhibit peaks that are characteristic of the compounds containing the  $[\text{CpW}(\text{CO})_3]$  group, which gives rise to the ions  $[\text{CpW}(\text{CO})_3]^+$  ( $m/z$  333, represented by  $^{184}\text{W}$ ),  $[\text{CpW}(\text{CO})_2]^+$  ( $m/z$  305),  $[\text{CpW}(\text{CO})]^+$  ( $m/z$  277), and  $[\text{CpW}]^+$  ( $m/z$  249). Similarly,  $[\text{Cp}^*\text{W}(\text{CO})_n]^+$  ( $n = 0\text{--}3$ ) contained peaks with low intensities are observed in the spectra of the Cp\* complexes.

The most abundant peak observed in the Cp complexes **3–6** and **9** corresponds to  $[\text{CpW}(\text{CO})_2\text{X}]^+$ , whereas for complexes **1**, **2**, **7** and **8**, the most abundant peak corresponds to  $[\text{CpWX}]^+$ . Due to the tungsten isotopes, the most abundant peak for complex **10** could not be assigned unambiguously, but is most likely to be  $[\text{CpW}(\text{CO})\text{X}]^+$ . All of the most abundant peaks observed include W–X fragments, which is a good indication that the interaction between the halogen and tungsten can exist in these haloalkyl complexes, particularly after CO is lost from the molecular ion. Such interaction could be postulated as shown in Scheme 3.

All the complexes fragment according to three main pathways as illustrated in Scheme 4 for complex **6**.

#### 2.2.5. Thermal properties of $[\text{CpW}(\text{CO})_3\{(\text{CH}_2)_n\text{Br}\}]$

The thermal properties of complexes  $[\text{CpW}(\text{CO})_3\{(\text{CH}_2)_n\text{Br}\}]$  ( $n = 3$ , **1**; and  $n = 4$ , **2**) were studied by DSC and TGA. The DSC traces of **1** and **2** recorded over the range  $40\text{--}300^\circ\text{C}$  under nitrogen and are shown in Fig. 1. The upper trace for **1** shows an endothermic peak at  $109^\circ\text{C}$ , which corresponds to the melting of the sample, by comparison with the hot-stage microscopy results. The exothermic peak at  $194^\circ\text{C}$  corresponds to

Table 7  
Mass spectral data for  $[\text{CpW}(\text{CO})_3\{(\text{CH}_2)_n\text{X}\}]$

Ion <sup>a</sup>	Relative peak intensities <sup>b</sup> (%)										
	<i>n</i> =	3		4		5		6		7	
		X =	Br	I	Br	I	Br	I	Br	I	Br
M		11	15	23	31	23	20	14	5	3	9
M–CO		12	24	0	0	2	4	5	0	4	7
M–3CO <sup>c</sup>		12	7	80	73	0	0	0	0	0	0
M–(CH <sub>2</sub> ) <sub><i>n</i></sub>		0	2	0	0	30	0	28	0	0	0
M–HX		0	0	27	3	5	58	0	0	0	0
M–(CH <sub>2</sub> ) <sub><i>n</i></sub> X		60	24	12	61	17	20	81	60	49	16
M–CO–(CH <sub>2</sub> ) <sub><i>n</i></sub>		52	100	80	82	100	60	100	100	100	69
M–CO–(CH <sub>2</sub> ) <sub><i>n</i></sub> X		37	41	53	71	56	45	56	83	62	48
M–CO–HX		12	22	0	41	0	0	0	66	0	100 <sup>d</sup>
M–2CO–(CH <sub>2</sub> ) <sub><i>n</i></sub>		65	46	93	73	0	54	84	99	79	100 <sup>d</sup>
M–2CO–(CH <sub>2</sub> ) <sub><i>n</i></sub> X		0	37	46	58	55	46	52	82	57	42
M–2CO–HX		10	44	0	61	8	43	0	89	0	88 <sup>e</sup>
M–3CO–(CH <sub>2</sub> ) <sub><i>n</i></sub> X		40	66	61	79	74	65	59	94	59	46
M–3CO–HX		18	20	0	0	4	0	13	0	24	5
M–(CH <sub>2</sub> ) <sub><i>n</i></sub> –CO <sub>2</sub>		13	11	0	0	17	11	2	0	0	0
M–(CH <sub>2</sub> ) <sub><i>n</i></sub> –X–CO <sub>2</sub>		24	37	0	0	9	16	2	0	0	0
M–(CH <sub>2</sub> ) <sub><i>n</i></sub> X–CO <sub>2</sub> –CO		15	29	4	3	13	0	8	0	0	0
M–(CH <sub>2</sub> ) <sub><i>n</i></sub> X–CO <sub>2</sub> –CpH		28	33	0	27	24	15	0	0	0	0
M–(CH <sub>2</sub> ) <sub><i>n</i></sub> X–CO <sub>2</sub> –CO–CpH		10	14	0	0	6	8	0	0	0	0
CpWX		100	91	100	100	0	100	81	93	56	88 <sup>e</sup>
WX		12	0	4	0	9	0	5	0	0	0

<sup>a</sup> M =  $[\text{CpW}(\text{CO})_3\{(\text{CH}_2)_n\text{X}\}]$ ; all ions have a single positive charge; ion refers to probable assignment.

<sup>b</sup> Peak intensities are relative to the base peak at *m/z* 328/330 due to  $[\text{CpWBr}]^+$  (calculations based on the most abundant peaks for all ions) for complexes X = Br, *n* = 3 and 4, *m/z* 376  $[\text{CpWI}]^+$  for X = I, *n* = 4 and 5; *m/z* 384/386 due to  $[\text{CpW}(\text{CO})_2\text{Br}]^+$  for complexes X = Br, *n* = 5–7, *m/z* 432 due to  $[\text{CpW}(\text{CO})_2\text{I}]^+$  for complexes X = I, *n* = 3 and 6; *m/z* 403 for X = I, *n* = 7.

<sup>c</sup> No ions corresponding to M–2CO, M–2CO–Cp, M–CO–Cp or M–3CO–Cp observed.

<sup>d</sup> These ions cannot be distinguished.

<sup>e</sup> These ions cannot be distinguished.

the decomposition of the complex. This can be seen from the TGA results (Fig. 2), which show a significant mass loss at this temperature.

The DSC trace for complex **2** shows three endothermic peaks at 62, 68 and 72°C, which by comparison with the hot-stage microscopy results, are assigned to the melting points of the sample. The presence of more than one peak in the melting range of **2** suggests that this complex may exist in several crystalline forms or phases. Further support for this is obtained by checking the IR and <sup>1</sup>H-NMR spectra of the sample after heating the sample to melting under nitrogen. Thus, the IR and <sup>1</sup>H-NMR spectra of the melted sample are the same as the IR and <sup>1</sup>H-NMR spectra of the pre-heated sample, although the color of the melted sample is slightly darker. In addition, the TGA also shows no decomposition over the range 40–190°C. The exothermic peak at 213°C on the DSC trace of **2** is assigned to the decomposition of the complex. This is seen from the TGA results, which show a significant mass loss at this temperature.

The decomposition temperature for **2** is ca. 10°C higher than that of **1**. This could be due to the alkyl chain length and the interaction between the tungsten and halogen as discussed in previous sections.

### 2.2.6. Electrochemical behavior of some haloalkyl complexes

The electrochemical properties of the haloalkyl complexes **1**, **8**, and **14** were studied under argon in acetonitrile solution at r.t. The oxidation potentials of these complexes are summarized in Table 9.

The CV measurements show that these haloalkyl and hydroxyalkyl complexes undergo chemically irreversible oxidation in the range 0.44–0.66 V versus the ferrocene/ferrocenium (Fc/Fc<sup>+</sup>) couple. These results are very similar to those obtained for  $[\text{CpW}(\text{CO})_3(\text{CH}_2)_6\text{CH}_3]$  [22]. This indicates that the oxidation of these haloalkyl complexes takes place at the tungsten center and is independent of the halo group. The complex with the Cp\* ligand, **14**, was oxidized at a much less positive potential than similar complexes containing the Cp ligand, which is a direct indication that the tungsten center in the Cp\* complex is more electron rich than in the Cp complexes. This is due to the strong electron donating effect of the Cp\* ligand. Similar studies on the iron complexes  $[\text{CpFe}(\text{CO})_2(\text{CH}_2)_5\text{CH}_3]$  and  $[\text{CpFe}(\text{CO})_2\{(\text{CH}_2)_6\text{Br}\}]$  have shown [10] that their electrochemical behavior and redox potentials are affected neither by the hydrocarbon chain length nor by the

Table 8  
Mass spectral data for  $[\text{Cp}^*\text{W}(\text{CO})_3\{(\text{CH}_2)_n\text{X}\}]$

Ion <sup>a</sup>	Relative intensity <sup>b</sup> (%)			
	n = 3		4	
	X = Br	I	Br	I
M	100	48	100	99
M–CO	46	34	0	1
M–2CO	17	8	2 <sup>c</sup>	1 <sup>d</sup>
M–3CO	0	10	0	100 <sup>e</sup>
M–HX	10	0	0	6
M–(CH <sub>2</sub> ) <sub>n</sub>	3	11	2 <sup>c</sup>	1 <sup>d</sup>
M–(CH <sub>2</sub> ) <sub>n</sub> X	0	45	0	0
M–CO–(CH <sub>2</sub> ) <sub>n</sub>	0	0	0	100 <sup>e</sup>
M–CO–HX	44	78	0	0
M–CO–(CH <sub>2</sub> ) <sub>n</sub> X	18	100	11	0
M–2CO–(CH <sub>2</sub> ) <sub>n</sub>	0	0	0	84
M–2CO–HX	0	0	0	0
M–2CO–(CH <sub>2</sub> ) <sub>n</sub> X	67	73	11	8
M–3CO–HX	27	79	0	0
M–3CO–(CH <sub>2</sub> ) <sub>n</sub> X	38	19	13	10
Cp*WX	0	20	0	7

<sup>a</sup> M =  $[\text{Cp}^*\text{W}(\text{CO})_3\{(\text{CH}_2)_n\text{X}\}]$ ; all ions have a single positive charge; ion refers to probable assignment.

<sup>b</sup> Peak intensities are relative to the parent peak for complexes with n = 3, 4 and X = Br, relative to  $[\text{Cp}^*\text{W}(\text{CO})_2]$  for n = 3, X = I, and relative to  $[\text{Cp}^*\text{W}(\text{CH}_2)_4\text{I}]$  for n = 4, X = I.

<sup>c</sup> These ions cannot be distinguished.

<sup>d</sup> These ions cannot be distinguished.

<sup>e</sup> These ions cannot be distinguished.

groups. Given the fact that these tungsten complexes show similar chemistry in a range of reactions to that of the iron complexes [10], it is expected that the electrochemical behavior of these tungsten complexes  $[\text{Cp}^*\text{W}(\text{CO})_3\{(\text{CH}_2)_n\text{X}\}]$  is not likely to be affected by the alkyl chain length or the nature of the functional groups.

### 2.3. Reactivity of $[\text{Cp}^*\text{W}(\text{CO})_3\{(\text{CH}_2)_n\text{X}\}]$

#### 2.3.1. Reaction of $[\text{Cp}^*\text{W}(\text{CO})_3\{(\text{CH}_2)_3\text{Br}\}]$ , **1** and $[\text{Cp}^*\text{W}(\text{CO})_3\{(\text{CH}_2)_4\text{I}\}]$ , **7** with 3,5-dihydroxybenzyl alcohol

The reaction of  $[\text{Cp}^*\text{Ru}(\text{CO})_2\{(\text{CH}_2)_3\text{Br}\}]$  with 3,5-dihydroxybenzyl alcohol has been reported as the first step for the preparation of large ruthenium dendrimers [18,19]. We have carried out similar reactions with tungsten haloalkyl complexes. The reaction of **1** with

3,5-dihydroxybenzyl alcohol in refluxing acetone for 3 days, in the presence of  $\text{K}_2\text{CO}_3$  and 18-crown-6, gave predominately the bis-substituted product **15**, (51% yield) and a small amount of the mono-substituted product **16**, (3%). Both complexes were obtained as yellow solids after purification by column chromatography and recrystallization (Scheme 5).

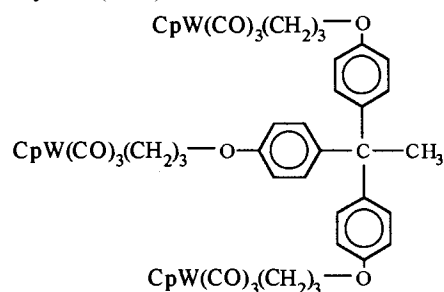
The reaction of  $[\text{Cp}^*\text{W}(\text{CO})_3(\text{CH}_2)_4\text{I}]$ , **7** with 3,5-dihydroxybenzyl alcohol was carried out similarly in refluxing acetone for 2 days, but gave only a low yield (24%) of the bis-substituted product, **17**.

Two bands are observed in the IR spectra of **15–17** at similar positions to those observed for the corresponding haloalkyl complexes. This suggests that the metal center is not affected by the reaction. The <sup>1</sup>H-NMR spectra of **15–17** show a CH<sub>2</sub>O proton triplet peaks at ca. δ 3.9 ppm, which confirms the conversion from the haloalkyl to the anticipated products. The complexes **15** and **16** can be easily distinguished by observation of the aromatic proton resonances and by integration, and also by observation of the phenolic OH proton peak at 4.7 ppm in the <sup>1</sup>H-NMR spectrum of **16**. Three separate proton resonances with equal integration are observed, in the region 6.2–6.4 ppm, in the <sup>1</sup>H-NMR spectrum of **16**, due to the inequivalence of these aromatic protons in the mononuclear complex. Two separate proton peaks with integration of 2:1 due to the aromatic protons are observed in the <sup>1</sup>H-NMR spectrum of **15**. Elemental analysis results confirm the formulae of the proposed complexes **15** and **16**.

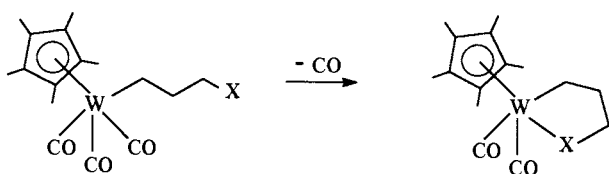
The thermal properties of **15** and **16** have also been studied. It is found that the mononuclear complex **16** is less thermally stable than the binuclear complex **15**. The melting points [DSC  $T_{\text{max}}(\text{endo})$ ] for **15** and **16** are 171 and 152°C, respectively, in agreement with the melting points observed on the hot-stage microscope. The decomposition points [DSC  $T_{\text{max}}(\text{exo})$ ] measured for **15** and **16** are 203 and 190°C, respectively.

#### 2.3.2. Reaction of $[\text{Cp}^*\text{W}(\text{CO})_3\{(\text{CH}_2)_3\text{Br}\}]$ , **1** with 1,1,1-tris(4'-hydroxyphenyl)ethane

The reaction of **1** with 1,1,1-tris(4'-hydroxyphenyl)ethane was also carried out in refluxing acetone for 3 days, in the presence of  $\text{K}_2\text{CO}_3$  and 18-crown-6, which gave the product **18** as shown below in good yield (61%).

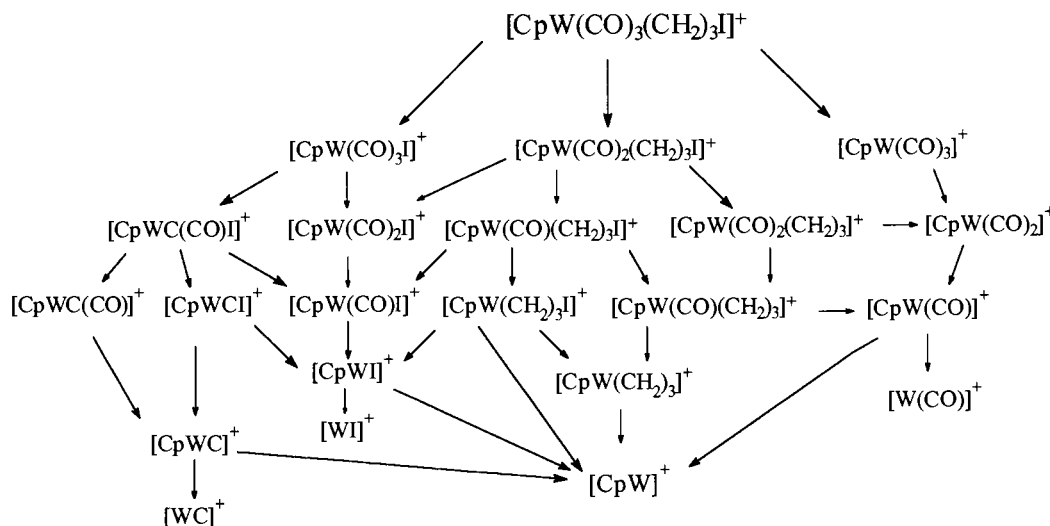


**18**



Scheme 3.





Scheme 4.

Complex **18** has been characterized by elemental analysis, IR,  $^1\text{H}$ - and  $^{13}\text{C}$ -NMR. The IR spectrum of **18** shows two  $\nu(\text{CO})$  bands at 2012 and 1913  $\text{cm}^{-1}$ , very similar to those observed in the IR spectra of **15**–**17**. The  $^1\text{H}$ -NMR spectrum of **18** shows a triplet at  $\delta$  3.85 ppm that corresponds to the  $\text{CH}_2$  attached to a phenoxy group. The integration of the protons also indicates the formula of the product being as anticipated.

### 2.3.3. Conversion of **15** to the benzyl bromide complex **19**

The benzyl alcohol complex **15** was reacted with  $\text{CBr}_4$  and  $\text{PPh}_3$  in THF at r.t. After purification by column chromatography and recrystallization, the benzyl bromide complex **19** was obtained in low yield (10%). This is in contrast to the similar reactions carried out for the iron and ruthenium complexes [10,17,18], which generally give benzyl bromide complexes in high yields (70–90%). This is likely to be due to the different metal employed. The complex **19** has also been characterized by IR and  $^1\text{H}$ -NMR. The IR spectrum of **19** shows the same bands as those for complex **15**. The  $^1\text{H}$ -NMR spectrum of **19** shows a characteristic single peak at  $\delta$  4.39 ppm, while all other peaks are found at the same positions as those in the  $^1\text{H}$ -NMR spectrum of **15**, which indicates the conversion of **15** to the anticipated product (Scheme 6).

### 2.3.4. Attempted preparation of a heterobimetallic complex containing W and Rh

A procedure reported [23] for the preparation of  $[\text{RhR}(\text{DH})_2(\text{py})]$  from  $[\text{RhCl}_2(\text{DH}_2)(\text{DH})]$  and  $\text{RX}$ , in the presence of  $\text{NaBH}_4$ , was followed in an attempt to prepare a heterobimetallic complex containing W

and Rh. Thus, the reaction of  $[\text{CpW}(\text{CO})_3\{(\text{CH}_2)_4\text{I}\}]$  and  $[\text{RhCl}_2(\text{DH}_2)(\text{DH})]$  in the presence of  $\text{NaBH}_4$  was conducted in a mixed solvent system of methanol/water/KOH/pyridine. After the reaction, none of the anticipated heterobimetallic complex could be observed. However, a yellow product was isolated in low yield (13%) in addition to some unreacted starting tungsten complex. This yellow product was identified as a new tungsten complex  $[\text{CpW}(\text{CO})_3\{(\text{CH}_2)_4\text{OCH}_3\}]$ , **20**, by elemental analysis, IR,  $^1\text{H}$ - and  $^{13}\text{C}$ -NMR as well as mass spectroscopy. Parent ions ( $m/z$  422) are observed in the mass spectrum of **20**.

Attempts were also made to prepare heterobinuclear complexes of W and Pt by the reaction of  $[\text{CpW}(\text{CO})_3\{(\text{CH}_2)_4\text{I}\}]$  with  $[\text{Pt}(\text{CH}_2=\text{CH}_2)(\text{PPh}_3)_2]$ , but these were unsuccessful. However, the reaction of  $[(\eta^5\text{-C}_5\text{R}_5)\text{W}(\text{CO})_3\{(\text{CH}_2)_n\text{I}\}]$  with  $[\text{PtMe}_2(\text{R}_2\text{-bipy})]$  ( $\text{R} = \text{H}, \text{CH}_3$ ) gave rise to a series of new heterobinuclear W/Pt complexes that have been reported elsewhere [17].

## 3. Conclusion

A series of  $\omega$ -haloalkyl complexes  $[(\eta^5\text{-C}_5\text{R}_5)\text{W}(\text{CO})_3\{(\text{CH}_2)_n\text{X}\}]$  ( $\text{R} = \text{H}, n = 3\text{--}7, \text{X} = \text{Br}$  and  $\text{I}; \text{R} = \text{CH}_3, n = 3, 4, \text{X} = \text{Br}$  and  $\text{I}$ ) has been synthesized and fully characterized. The characterization data obtained for these haloalkyl complexes support previous observations by other workers that there is an interaction between the metal and the  $\gamma$ -C–X bond in halopropyl transition metal complexes. The haloalkyl complexes have been used as precursors for the synthesis of binuclear and polynuclear complexes.

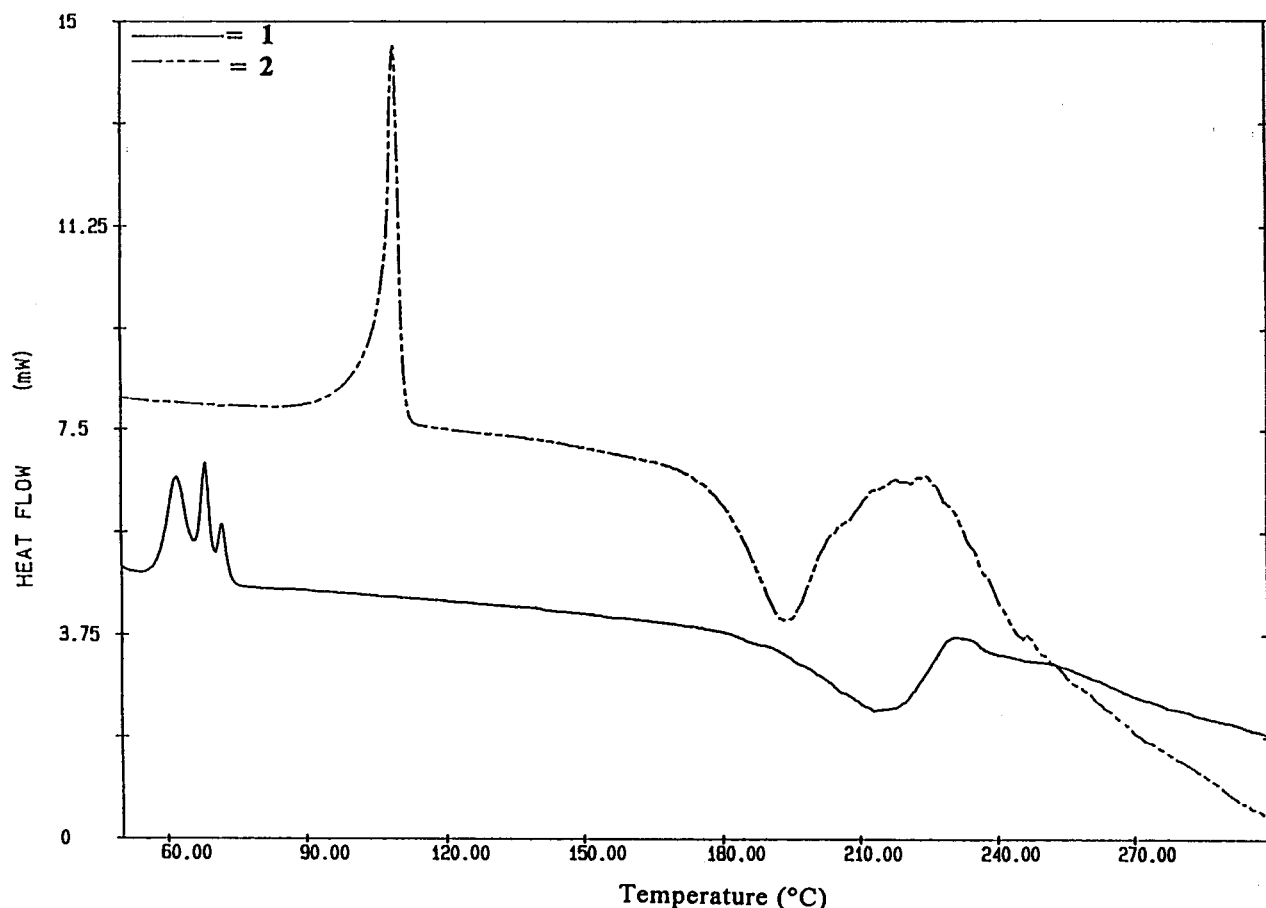


Fig. 1. DSC traces for the complexes **1** and **2** (scan rate =  $20^{\circ}\text{C min}^{-1}$ ).

#### 4. Experimental

All reactions were carried out under an atmosphere of high purity nitrogen using standard Schlenk tube techniques. Tetrahydrofuran (THF) and hexane were dried by distilling over sodium/benzophenone. Dichloromethane ( $\text{CH}_2\text{Cl}_2$ ) was distilled over anhydrous  $\text{CaCl}_2$ . Acetone was distilled over anhydrous  $\text{CaCl}_2$  or  $\text{K}_2\text{CO}_3$ . Acetonitrile was distilled over  $\text{P}_2\text{O}_5$ . Pyridine was dried over sodium hydroxide pellets. Methanol (MeOH) was distilled over molecular sieve (3A or 4A).  $[\text{Cp}^*\text{W}(\text{CO})_3]_2$  was obtained from Strem Chemical, USA and was used without further purification. The complexes  $[\text{Cp}^*\text{W}(\text{CO})_3]_2$  [24], 3,5-dihydroxybenzyl alcohol [25], and  $[\text{RhCl}_2(\text{DH}_2)(\text{DH})]$  [23] were prepared by literature methods. Alumina (BDH, active neutral, Brockman grade I) was deactivated before use. The dihaloalkanes (Aldrich) were used without purification.

Melting points were recorded on a Kofler hot-stage microscope (Reichert Thermovar) and are uncorrected. Differential scanning calorimetry (DSC) and thermal gravimetric analysis (TGA) were performed on a Perkin-Elmer PC Series 7 instrument under a nitrogen

atmosphere with a heating rate of 10 or  $20^{\circ}\text{C min}^{-1}$ . Microanalyses were performed by the University of Cape Town Microanalytical Laboratory. IR spectra were recorded either on a Perkin-Elmer 983 or a Paragon 1000 FT-IR spectrophotometer in solution cells with NaCl windows.

$^1\text{H-NMR}$  spectra were recorded on a Varian XR 200 (at 200 MHz) spectrometer or a Varian Unity 400 (at 400 MHz) spectrometer.  $^{13}\text{C-NMR}$  spectra were recorded on the Varian XR 200 (at 50 MHz) spectrometer or the Varian Unity 400 (at 100 MHz) spectrometer. The chemical shifts are relative to TMS (0 ppm) in the  $^1\text{H}$ - and  $^{13}\text{C}$ -NMR spectra, whereas the deuterated solvent signals were used as references and the chemical shifts adjusted accordingly. Low resolution mass spectra were recorded with a VG Micromass 16F spectrometer operated at 70 eV ionizing voltage and using an accelerating voltage of 4 kV.

Cyclic voltammetry (CV) was carried out on a BAS-100B electrochemical analyser in a one-compartment three-electrode system, consisting of  $\text{Ag}/\text{Ag}^+$  (0.01 M) as the reference electrode, platinum wire as the auxiliary electrode and a platinum disk electrode as the working electrode. The supporting electrolyte was a

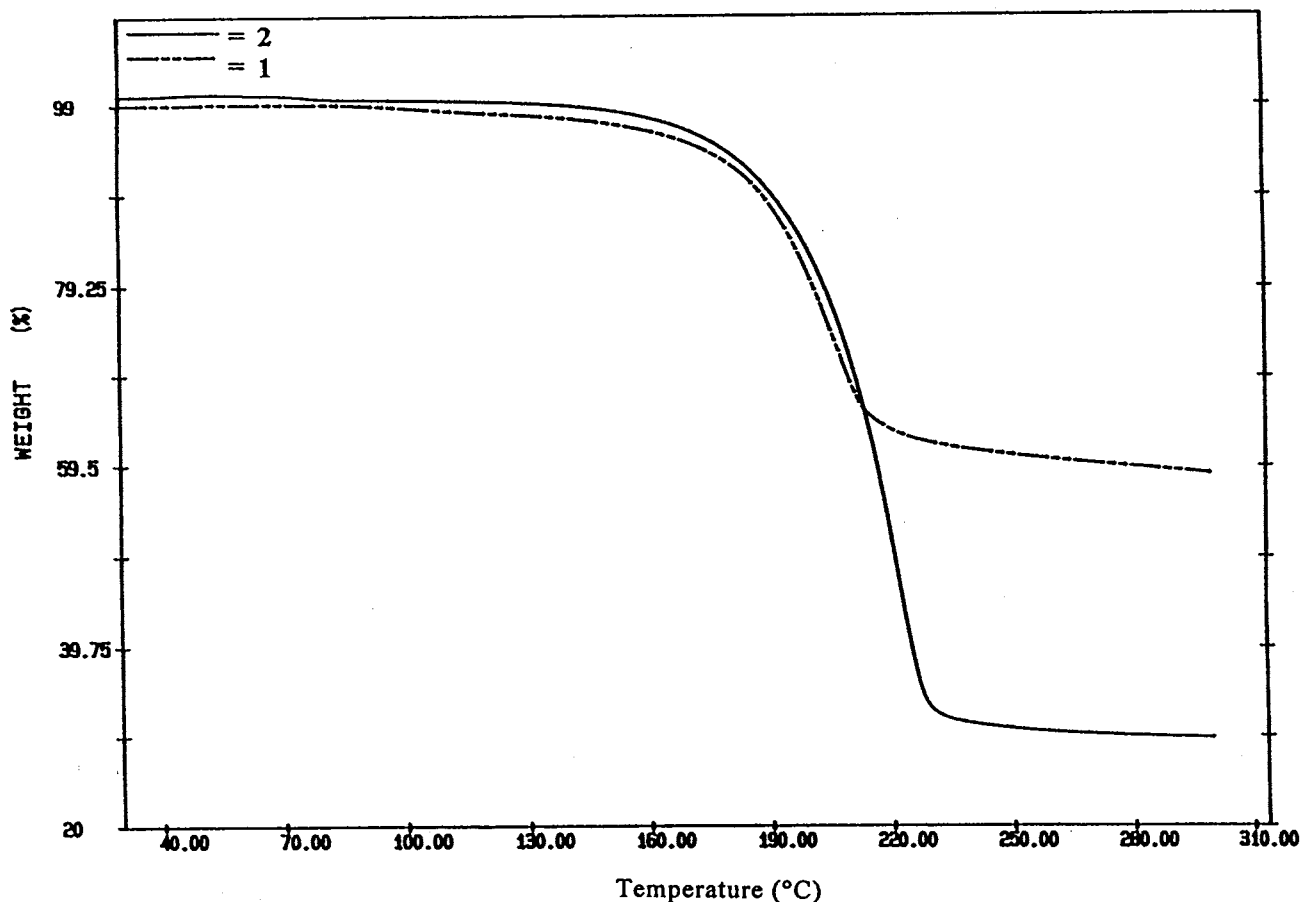
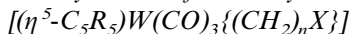


Fig. 2. TGA traces for the complexes **1** and **2** (scan rate = 20°C min<sup>-1</sup>).

solution of 0.1 M [NBu<sub>4</sub>][ClO<sub>4</sub>] in dry acetonitrile. The potentials *E* were recorded without IR compensation. All potentials reported are relative to the half-wave potential *E*<sub>1/2</sub> of the ferrocene/ferrocenium couple run under the same conditions. The experiments were performed on 1.0 mM solutions under an argon atmosphere at r.t. The platinum disk electrode was polished after every three runs.

#### 4.1. Synthesis of haloalkyl complexes



The preparation of complexes [CpW(CO)<sub>3</sub>{(CH<sub>2</sub>)<sub>3</sub>Br}] [**1**], [CpW(CO)<sub>3</sub>{(CH<sub>2</sub>)<sub>4</sub>Br}] [**1**], [Cp\*W(CO)<sub>3</sub>{(CH<sub>2</sub>)<sub>3</sub>Br}] [**14**], [CpW(CO)<sub>3</sub>{(CH<sub>2</sub>)<sub>4</sub>I}] [**20**] and [CpW(CO)<sub>3</sub>{(CH<sub>2</sub>)<sub>5</sub>I}] [**20**] has been reported in the literature, however, the procedures given here lead to better yields for these complexes. All other complexes synthesized in this work are new complexes.

##### 4.1.1. Synthesis of [CpW(CO)<sub>3</sub>{(CH<sub>2</sub>)<sub>3</sub>Br}], **1** [**1**]

A solution of Na[CpW(CO)<sub>3</sub>] (3.0 mmol), generated from [CpW(CO)<sub>3</sub>]<sub>2</sub> (1.00 g, 1.5 mmol) over Na/Hg (0.40 g Na, 4 ml Hg) in THF (20 ml) at r.t., was added dropwise over 5 min to 1,3-dibromopropane (1.20 g, 6.0

mmol) in THF (2 ml) with stirring at r.t. The reaction mixture was stirred for 44 h at r.t. to effect completion. The reaction was monitored by IR spectroscopy, based on the decrease of the ν(CO) bands of the anion [CpW(CO)<sub>3</sub>]<sup>-</sup> at 1894, 1790 and 1744 cm<sup>-1</sup>. The solvent was removed under reduced pressure and the residue was extracted with CH<sub>2</sub>Cl<sub>2</sub> (3 × 30 ml), filtered and the solvent removed. The residue was dissolved in a minimum amount of 10% CH<sub>2</sub>Cl<sub>2</sub>/hexane, then separated on an alumina column. Elution with hexane gave a yellow band which was concentrated, and cooled to -78°C to yield yellow crystals of the pure product **1** (0.90 g, 66%). The melting point, elemental analysis and physical characterization data of **1** (and others **2**–**14**) are given in the Section 2.

##### 4.1.2. Preparation of [CpW(CO)<sub>3</sub>{(CH<sub>2</sub>)<sub>4</sub>Br}], **2** [**1**]

This was prepared by the method described above for **1** with the following quantities of reagents: [CpW(CO)<sub>3</sub>]<sub>2</sub>, (0.57 g, 0.85 mmol), 1,4-dibromobutane (1.10 g, 4.9 mmol), and a reaction time of 114 h at r.t. Work-up as described above for **1**, gave **2** as yellow crystals (0.36 g, 45%).

Table 9  
Oxidation potentials for haloalkyl and hydroxyalkyl complexes measured under argon in 1.0 mM acetonitrile solution containing 0.1 M  $[\text{NBu}_4^+]\text{ClO}_4^-$  at r.t.

Compound	$E_a$ (V vs. Fc/Fc <sup>+</sup> )	Scan rate (mV s <sup>-1</sup> )	Number of measurements
1	0.66	500	2
8	0.63	100	3
14	0.44	100	3
$[\text{Wp}(\text{CH}_2)_6\text{CH}_3]^a$	0.56	200	3
$[\text{Wp}(\text{CH}_2)_6\text{CH}_3]^a$	0.61	100	3

<sup>a</sup> Results from [22].

#### 4.1.3. Preparation of $[\text{CpW}(\text{CO})_3\{(\text{CH}_2)_5\text{Br}\}]$ , **3**

This was prepared by the method described above for **1** with the following quantities of reagents:  $[\text{CpW}(\text{CO})_3]_2$ , (0.80 g, 1.2 mmol), 1,5-dibromopentane (1.04 g, 4.5 mmol), and a reaction time of 10 days at r.t. Work-up as described above for **1**, gave **3** as yellow crystals (0.60 g, 50%).

#### 4.1.4. Preparation of $[\text{CpW}(\text{CO})_3\{(\text{CH}_2)_6\text{Br}\}]$ , **4**

This was prepared by the method described above for **1** with the following quantities of reagents:  $[\text{CpW}(\text{CO})_3]_2$ , (0.45 g, 0.68 mmol), 1,6-dibromohexane (0.38 g, 1.56 mmol), and a reaction time of 16 h under refluxing condition. Work-up as described above for **1**, elution with hexane and gradually increasing the polarity by addition of diether ether, and recrystallization from hexane at  $-20^\circ\text{C}$ , gave **4** as yellow crystals (0.33 g, 49%).

#### 4.1.5. Preparation of $[\text{CpW}(\text{CO})_3\{(\text{CH}_2)_7\text{Br}\}]$ , **5**

This was prepared by the method described above for **4** with the following quantities of reagents:  $[\text{CpW}(\text{CO})_3]_2$ , (0.50 g, 0.75 mmol), 1,7-dibromoheptane (0.46 g, 1.78 mmol), and a reaction time of 16 h under refluxing condition. Work-up as described above for **4** and recrystallization from hexane at  $-78^\circ\text{C}$ , gave **5** as yellow crystals (0.28 g, 37%).

#### 4.1.6. Preparation of $[\text{CpW}(\text{CO})_3\{(\text{CH}_2)_3\text{I}\}]$ , **6**

Sodium iodide (0.10 g, 0.68 mmol) was added to a solution of **1** (0.16 g, 0.34 mmol) in acetone (10 ml). The mixture was stirred at r.t. for 27 h. The solvent was removed under reduced pressure and the residue extracted with hexane. The combined extracts were filtered, concentrated and transferred to an alumina column. Elution with hexane gave a yellow band, which was concentrated, filtered and recrystallized from hexane at  $-20^\circ\text{C}$ . The product **6** (0.12 g, 70%) was obtained as yellow crystals.

#### 4.1.7. Preparation of $[\text{CpW}(\text{CO})_3\{(\text{CH}_2)_4\text{I}\}]$ , **7** [20]

This was prepared by the method described above for **1** with the following quantities of reagents:  $[\text{CpW}(\text{CO})_3]_2$ , (1.00 g, 1.5 mmol), 1,4-diiodobutane (1.10 g,

3.5 mmol), and a reaction time of 6 h at r.t. Work-up as described above for **1**, and recrystallization from hexane at  $-20^\circ\text{C}$  gave **7** as yellow crystals (0.87 g, 56%).

#### 4.1.8. Preparation of $[\text{CpW}(\text{CO})_3\{(\text{CH}_2)_5\text{I}\}]$ , **8** [20]

This was prepared by the method described above for **6** with the following quantities of reagents: **3** (0.30 g, 0.62 mmol), NaI (0.30 g, 1.8 mmol), and a reaction time of 30 h. Work-up as described above for **6**, and recrystallization from acetone/hexane at  $-20^\circ\text{C}$  for 4 days gave **8** as yellow crystals (0.21 g, 63%).

#### 4.1.9. Preparation of $[\text{CpW}(\text{CO})_3\{(\text{CH}_2)_6\text{I}\}]$ , **9**

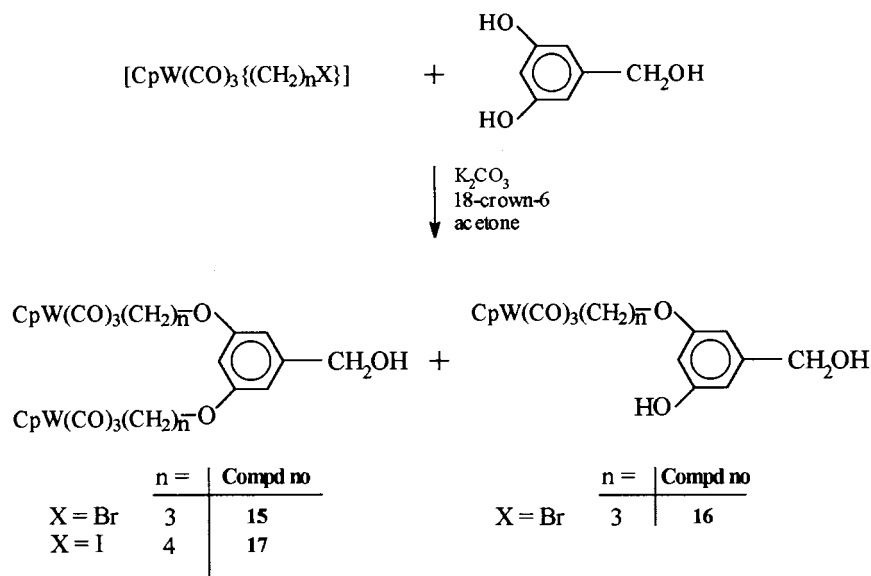
This was prepared by the method described above for **6**, with the following quantities of reagents: **4** (0.17 g, 0.35 mmol), NaI (0.12 g, 0.8 mmol), and a reaction time of 36 h. Work-up as described above for **6**, and recrystallization from hexane at  $-20^\circ\text{C}$  gave **9** as yellow crystals (0.12 g, 62%).

#### 4.1.10. Preparation of $[\text{CpW}(\text{CO})_3\{(\text{CH}_2)_7\text{I}\}]$ , **10**

This was prepared by the method described above for **6** with the following quantities of reagents: **5** (0.15 g, 0.30 mmol), NaI (0.11 g, 0.7 mmol), and a reaction time of 36 h. Work-up as described above for **6**, and recrystallization from hexane at  $-78^\circ\text{C}$  gave **10** as yellow crystals (0.09 g, 57%).

#### 4.1.11. Preparation of $[\text{Cp}^*\text{W}(\text{CO})_3\{(\text{CH}_2)_3\text{Br}\}]$ , **11** [14]

A solution of  $\text{Na}[\text{Cp}^*\text{W}(\text{CO})_3]$  (0.64 mmol, generated from  $[\text{Cp}^*\text{W}(\text{CO})_3]_2$  (0.26 g, 0.32 mmol) over Na/Hg (0.16 g Na, 2 ml Hg) in THF (15 ml) at r.t. for 1 h), was added dropwise to a solution of 1,3-dibromopropane (0.26 g, 1.28 mmol) in THF (2 ml) at  $0^\circ\text{C}$  with rapid stirring. The reaction mixture was stirred for 18 h at r.t.. After this, the solvent was removed under reduced pressure, leaving a yellow residue. This was extracted with diether ether, concentrated and chromatographed on an alumina column. Elution with hexane gave a fast-moving yellow band, which was collected. The solvent was removed to give a yellow oily product. Recrystallization from pentane at  $-78^\circ\text{C}$  gave **11** as a yellow crystalline solid (0.23 g, 68%).



Scheme 5.

#### 4.1.12. Preparation of $[Cp^*W(CO)_3\{(CH_2)_4Br\}]$ , **12**

This was prepared similarly as above from  $[Cp^*W(CO)_3]_2$  (0.48 g, 0.60 mmol) and 1,4-dibromobutane (0.39 g, 1.8 mmol), and a reaction time of 18 h. Recrystallization from hexane at  $-78^\circ\text{C}$  gave **12** as a yellow crystalline solid (0.40 g, 62%).

#### 4.1.13. Preparation of $[Cp^*W(CO)_3\{(CH_2)_3I\}]$ , **13**

This was prepared by the method described previously for the preparation of **6** with the following quantities of reagents: **11** (0.17 g, 0.32 mmol), NaI (0.14 g, 0.93 mmol) and a reaction time of 45 h. Recrystallization from hexane at  $-78^\circ\text{C}$  gave **13** as yellow crystals (0.15 g, 78%).

#### 4.1.14. Preparation of $[Cp^*W(CO)_3\{(CH_2)_4I\}]$ , **14**

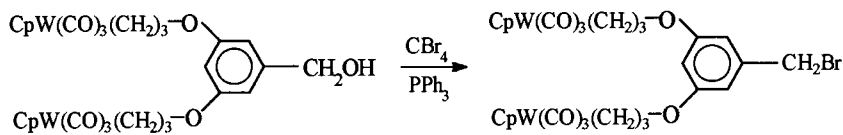
This was prepared by the method described for the preparation of **13** with the following quantities of reagents: **12** (0.25 g, 0.46 mmol), NaI (0.26 g, 1.7 mmol) and a reaction time of 42 h. Recrystallization from hexane at  $-78^\circ\text{C}$  gave **14** as yellow crystals (0.19 g, 71%).

### 4.2. Reactivity of haloalkyl complexes

#### 4.2.1. Reaction of $[Cp^*W(CO)_3\{(CH_2)_3Br\}]$ , **1** with 3,5-dihydroxybenzyl alcohol to give the benzyl alcohol complexes $[\{Cp^*W(CO)_3(CH_2)_3O-\}_2(C_6H_3)-CH_2OH]$ , **15** and $[\{Cp^*W(CO)_3(CH_2)_3O-\}\{C_6H_3(OH)\}-CH_2OH]$ , **16**

A mixture of **1** (2.05 g, 4.52 mmol), 3,5-dihydroxybenzyl alcohol (0.31 g, 2.2 mmol), 18-crown-6 (0.116 g, 0.45 mmol) and  $K_2CO_3$  (0.91 g, 6.6 mmol) in acetone (70 ml) was heated to reflux and stirred vigorously for 67 h. The reaction was protected from light by alu-

minium foil and monitored by TLC (alumina, 30%  $CH_2Cl_2$ /hexane). The reaction mixture was then allowed to cool and the solvent removed under reduced pressure, leaving a yellow-orange residue. The residue was extracted with  $CH_2Cl_2$  three times. The combined extracts were filtered, concentrated and then transferred to an alumina column. The first yellow band was eluted with 70%  $CH_2Cl_2$ /hexane, which gave presumably unreacted starting material in very small amount. Eluting with  $CH_2Cl_2$  and gradually increasing the polarity to 10% MeOH/ $CH_2Cl_2$  gave additional two yellow bands. The major band was collected, and the solvent was removed, giving a yellow solid product. The yellow product was then recrystallized from  $CH_2Cl_2$ /hexane to give the yellow crystalline product **15**, (1.02 g, 51% based on 3,5-dihydroxybenzyl alcohol); m.p.  $155-157^\circ\text{C}$  (Found: C, 38.97; H, 3.14%;  $C_{29}H_{28}O_9W_2$  requires: C, 39.21; H, 3.18%), IR  $\nu(CO)$  ( $CH_2Cl_2$ ): 2013s, 1913s  $\text{cm}^{-1}$ ;  $^1\text{H-NMR}$  ( $CDCl_3$ )  $\delta$  (ppm): 6.49 (2 H, d,  $^4J(\text{HH})$  2.4 Hz, aromatic), 6.37 (1 H, t,  $^4J(\text{HH})$  2.4 Hz, aromatic), 5.41 (10 H, s, Cp), 4.61 (2 H, s,  $CH_2OH$ ), 3.86 (4 H, t,  $^3J(\text{HH})$  6.4 Hz,  $CH_2OAr$ ), 2.01 (4 H, m,  $CH_2CH_2CH_2$ ), 1.56 (4 H, m,  $WCH_2$ );  $^{13}\text{C-NMR}$  ( $CDCl_3$ )  $\delta$  (ppm): 228.57, 217.37 (CO), 160.52, 143.19, 105.10, 100.52 (Ar), 91.57 (Cp), 71.96 ( $CH_2OAr$ ), 65.48 ( $CH_2OH$ ), 36.22 ( $CH_2CH_2CH_2$ ),  $-16.43$  ( $WCH_2$ ). The minor yellow band was also collected, which after removing solvent and recrystallization from  $CH_2Cl_2$ /hexane, gave another yellow product **16** (0.071 g, 3%); m.p.  $141-144^\circ\text{C}$  (Found: C, 41.75; H, 3.51%;  $C_{18}H_{18}O_6W$  requires: C, 42.05; H, 3.53%), IR  $\nu(CO)$  ( $CH_2Cl_2$ ): 2013s, 1911s  $\text{cm}^{-1}$ ;  $^1\text{H-NMR}$  ( $CDCl_3$ )  $\delta$  (ppm): 6.49 (1 H, d,  $^4J(\text{HH})$  2.4 Hz, aromatic), 6.42 (1 H, m, aromatic) 6.31 (1 H, t,  $^4J(\text{HH})$  2.4 Hz, aromatic), 5.41 (5 H, s, Cp), 4.92 (1 H, s,  $ArOH$ ), 4.60 (2 H, s,



19

Scheme 6.

$\text{CH}_2\text{OH}$ ), 3.85 (2 H, t,  $^3J(\text{HH})$  6.4 Hz,  $\text{CH}_2\text{OAr}$ ), 2.01 (2 H, m,  $\text{CH}_2\text{CH}_2\text{CH}_2$ ), 1.56 (2 H, m,  $\text{WCH}_2$ ), 1.25 (1 H, s,  $\text{CH}_2\text{OH}$ ).

#### 4.2.2. Reaction of $[\text{CpW(CO)}_3\{(\text{CH}_2)_4\text{I}\}]$ , **7** with 3,5-dihydroxybenzyl alcohol to give

##### $[\{\text{CpW(CO)}_3(\text{CH}_2)_4\text{O}\}_2(\text{C}_6\text{H}_3)-\text{CH}_2\text{OH}]$ , **17**

A mixture of **7** (0.13 g, 0.26 mmol), 3,5-dihydroxybenzyl alcohol (0.018 g, 0.13 mmol), 18-crown-6 (0.01 g, 0.04 mmol) and  $\text{K}_2\text{CO}_3$  (0.09 g, 0.66 mmol) in acetone (20 ml) was heated to reflux and stirred vigorously for 48 h. Work-up as described above for **15** gave the complex **17** (0.029 g, 24%) as a yellow solid; IR  $\nu(\text{CO})$  ( $\text{CH}_2\text{Cl}_2$ ): 2011s, 1911s  $\text{cm}^{-1}$ ;  $^1\text{H-NMR}$  ( $\text{CDCl}_3$ )  $\delta$  (ppm): 6.51 (2 H, d,  $^4J(\text{HH})$  2.4 Hz, aromatic), 6.38 (1 H, t,  $^4J(\text{HH})$  2.4 Hz, aromatic), 5.38 (10 H, s, Cp), 4.62 (2 H, s,  $\text{CH}_2\text{OH}$ ), 3.96 (4 H, t,  $^3J(\text{HH})$  6.4 Hz,  $\text{CH}_2\text{OAr}$ ), 1.76 (8 H, m,  $\text{CH}_2\text{CH}_2\text{CH}_2\text{CH}_2$ ), 1.56 (4 H, m,  $\text{WCH}_2$ ), 1.25 (1 H, s,  $\text{CH}_2\text{OH}$ );  $^{13}\text{C-NMR}$  ( $\text{CDCl}_3$ )  $\delta$  (ppm): 228.79, 217.51 (CO), 160.52, 143.17, 105.15, 100.68 (Ar), 91.49 (Cp), 67.29 ( $\text{CH}_2\text{OAr}$ ), 65.47 ( $\text{CH}_2\text{OH}$ ), 35.03, 33.08 ( $\text{CH}_2\text{CH}_2\text{CH}_2\text{CH}_2$ ), -11.24 ( $\text{WCH}_2$ ). Satisfactory elemental analysis results were not obtained for this compound.

#### 4.2.3. Reaction of $[\text{CpW(CO)}_3\{(\text{CH}_2)_3\text{Br}\}]$ , **1** with 1,1,1-tris(4'-hydroxyphenyl)ethane to give the tri-nuclear tungsten complex

##### $[\{\text{CpW(CO)}_3(\text{CH}_2)_3\text{O}-(\text{C}_6\text{H}_4)_3\}_3-\text{CCH}_3]$ , **18**

A mixture of **1** (0.26 g, 0.57 mmol), 1,1,1-tris(4'-hydroxyphenyl)ethane (0.052 g, 0.17 mmol), 18-crown-6 (0.012 g, 0.05 mmol) and  $\text{K}_2\text{CO}_3$  (0.15 g, 1.1 mmol) in acetone (20 ml) was heated to reflux and stirred vigorously for 72 h. Work-up as described above for **15** gave **18** (0.050 g, 61%); m.p. 85–88°C (Found: C, 44.86; H, 4.03%;  $\text{C}_{53}\text{H}_{48}\text{O}_{12}\text{W}_3$  requires: C, 44.56; H, 3.39%), IR  $\nu(\text{CO})$  ( $\text{CH}_2\text{Cl}_2$ ): 2012s, 1913s  $\text{cm}^{-1}$ ;  $^1\text{H-NMR}$  ( $\text{CDCl}_3$ )  $\delta$  (ppm): 6.96 (6 H, d,  $^3J(\text{HH})$  8.8 Hz), 6.75 (6H, d,  $^3J(\text{HH})$  8.8 Hz), 5.40 (15 H, s, Cp), 3.85 (6 H, t,  $^3J(\text{HH})$  6.4 Hz), 2.09 (3 H, s,  $\text{CH}_3$ ), 2.00 (6 H, m,  $\text{CH}_2\text{CH}_2\text{CH}_2$ ), 1.57 (6 H, m,  $\text{WCH}_2$ );  $^{13}\text{C-NMR}$  ( $\text{CDCl}_3$ )  $\delta$  (ppm): 228.49, 217.21 (CO), 157.02, 141.66, 129.54, 113.61 (Ar), 91.48 (Cp), 71.80 ( $\text{CH}_2\text{O}$ ), 50.55 ( $\text{CCH}_3$ ), 36.27 ( $\text{WCH}_2\text{CH}_2$ ), 30.73 ( $\text{CCH}_3$ ), -16.36 ( $\text{WCH}_2$ ).

#### 4.2.4. Conversion of the benzyl alcohol complex **15** to the benzyl bromide complex $[\{\text{CpW(CO)}_3(\text{CH}_2)_3\text{O}\}_2(\text{C}_6\text{H}_3)-\text{CH}_2\text{Br}]$ , **19**

To a solution of **15** (0.13 g 0.15 mmol) in THF (2 ml)  $\text{PPh}_3$  (0.05g, 0.19 mmol) and  $\text{CBr}_4$  (0.06 g, 0.19 mmol) were added. The reaction mixture was stirred for 15 min at r.t. Additional  $\text{PPh}_3$  (0.05g, 0.19 mmol) and  $\text{CBr}_4$  (0.06 g, 0.19 mmol) were added to the reaction mixture and the reaction continued for another 25 min. Monitoring the reaction by TLC showed that complete conversion of the starting complex had occurred. Distilled water (10 ml) was added to quench the reaction. The resulting mixture was extracted twice with  $\text{CH}_2\text{Cl}_2$  and the combined extracts were dried ( $\text{Mg}_2\text{SO}_4$ ), concentrated and transferred to an alumina column. The first yellow band, eluted with 30%  $\text{CH}_2\text{Cl}_2$ /hexane, was very unstable and turned black soon after it was eluted. The second yellow band gave an oily solid. Recrystallization from  $\text{CH}_2\text{Cl}_2$ /hexane and drying under high vacuum gave **19** (0.014 g, 10%) as a yellow-brown solid, m.p. 96–105°C (Found: C, 37.48; H, 3.12%;  $\text{C}_{29}\text{H}_{28}\text{O}_8\text{BrW}_2$  requires: C, 36.62; H, 2.86%), IR  $\nu(\text{CO})$  ( $\text{CH}_2\text{Cl}_2$ ): 2013s, 1913s  $\text{cm}^{-1}$ ;  $^1\text{H-NMR}$  ( $\text{CDCl}_3$ )  $\delta$  (ppm): 6.49 (2 H, d,  $^4J(\text{HH})$  2.4 Hz, aromatic), 6.35 (1 H, t,  $^4J(\text{HH})$  2.4 Hz, aromatic), 5.40 (10 H, s, Cp), 4.39 (2 H, s,  $\text{CH}_2\text{Br}$ ), 3.85 (4 H, t,  $^3J(\text{HH})$  6.4 Hz,  $\text{CH}_2\text{OAr}$ ), 2.00 (4 H, m,  $\text{CH}_2\text{CH}_2\text{CH}_2$ ), 1.55 (4 H, m,  $\text{WCH}_2$ ).

#### 4.2.5. Attempted reaction of $[\text{RhCl}_2(\text{DH}_2)(\text{DH})]$ with $[\text{CpW(CO)}_3\{(\text{CH}_2)_4\text{I}\}]$ , **7**: isolation of $[\text{CpW(CO)}_3\{(\text{CH}_2)_4\text{OCH}_3\}]$ , **20**

This procedure is similar to that reported for the synthesis of  $[\text{Rh}(\text{DH})_2(\text{py})]$  [23].  $[\text{RhCl}_2(\text{DH}_2)(\text{DH})]$  (0.12 g, 0.30 mmol) was suspended in MeOH (18 ml). The suspension was treated with 50% aqueous KOH solution (3 ml) at r.t. followed by a solution of  $\text{NaBH}_4$  (0.012 g, 0.30 mmol) in MeOH (2 ml). An immediate color change from yellow to black indicated that the reduction of Rh(III) to Rh(I) had occurred. After 30 min, **7** (0.165 g, 0.32 mmol) was added to the Rh(I) solution at r.t.. The color of the reaction mixture gradually turned to yellow. After 30 min, pyridine (0.03 g, 0.38 mmol) was added to the mixture and the solution stirred for further 40 min. The solvent was removed under reduced pressure, leaving a yellow oil. The oil was dissolved in  $\text{CH}_2\text{Cl}_2$  and the solution washed with water and  $\text{NH}_4\text{Cl}$  solution. The organic

layer was separated, the aqueous layer was washed once with  $\text{CH}_2\text{Cl}_2$ . The combined  $\text{CH}_2\text{Cl}_2$  solution was dried ( $\text{Mg}_2\text{SO}_4$ ), concentrated and dried, to give a yellow solid. This solid was further purified by chromatography on an alumina column, eluted with hexane then gradually increase the polarity by slow adding ether. The first yellow fraction was unreacted starting material  $[\text{CpW}(\text{CO})_3\{(\text{CH}_2)_4\text{I}\}]$ , based on its TLC and IR. The second yellow band, after recrystallization from hexane, gave **20** (0.032 g, 25%), m.p. 59–60°C (Found: C, 37.77; H, 3.91%; EI-MS,  $m/z$  422 ( $\text{M}^+$ ),  $\text{C}_{13}\text{H}_{16}\text{O}_4\text{W}$  requires: C, 37.17; H, 3.84%; M, 420), IR  $\nu(\text{CO})$  (hexane): 2016s, 1926vs  $\text{cm}^{-1}$ ;  $^1\text{H-NMR}$  ( $\text{CDCl}_3$ )  $\delta$  (ppm): 5.39 (5 H, s, Cp), 3.38 (2 H, t,  $^3J(\text{HH})$  6.4,  $\text{CH}_2\text{O}$ ), 3.34 (3 H, s,  $\text{CH}_3\text{O}$ ), 1.58 (6 H, m,  $\text{WCH}_2\text{CH}_2\text{CH}_2$ ).  $^{13}\text{C-NMR}$  ( $\text{CDCl}_3$ )  $\delta$  (ppm): 228.91, 217.45 (CO), 91.47 (Cp), 72.27 ( $\text{CH}_2\text{O}$ ), 58.49 ( $\text{CH}_3\text{O}$ ), 35.60, 33.30 ( $\text{CH}_2\text{CH}_2\text{CH}_2\text{CH}_2$ ), –10.69 ( $\text{WCH}_2$ ).

### Acknowledgements

We thank the University of Cape Town, SASOL and the Foundation for Research and Development for support and Johnson Matthey for the generous loan of platinum metal salts. We also thank Dr A.T. Hutton for assisting with the electrochemical measurements.

### References

- [1] R.B. King, M.B. Bisnette, *J. Organomet. Chem.* 7 (1967) 311.
- [2] H.B. Friedrich, J.R. Moss, *Adv. Organomet. Chem.* 33 (1991) 235.
- [3] J.R. Moss, *J. Organomet. Chem.* 231 (1982) 229.
- [4] J.R. Moss, S. Pelling, *J. Organomet. Chem.* 236 (1982) 221.
- [5] H.B. Friedrich, P.A. Makhsha, J.R. Moss, B.K. Williamson, *J. Organomet. Chem.* 384 (1990) 325.
- [6] H.B. Friedrich, K.P. Finch, M.A. Gafoor, J.R. Moss, *Inorg. Chim. Acta* 206 (1993) 225.
- [7] S. Pelling, C. Botha, J.R. Moss, *J. Chem. Soc. Dalton Trans.* (1983) 1495.
- [8] H.B. Friedrich, J.R. Moss, *J. Organomet. Chem.* 453 (1993) 85.
- [9] J.R. Moss, M.L. Niven, P.M. Stretch, *Inorg. Chim. Acta* 119 (1986) 177.
- [10] Y.-H. Liao, Ph.D. Thesis, University of Cape Town, South Africa, 1994.
- [11] J.R. Moss, *Trends Organomet. Chem.* 1 (1994) 211.
- [12] N.A. Bailey, P.L. Chell, C.P. Manuel, A. Mukhopadhyay, D. Rogers, H.E. Tabbron, M.J. Winter, *J. Chem. Soc. Dalton Trans.* (1983) 2397.
- [13] H. Adams, N.A. Bailey, M.J. Winter, *J. Chem. Soc. Dalton Trans.* (1984) 273.
- [14] N.A. Bailey, D.A. Dunn, C.N. Foxcroft, G.R. Harrison, M.J. Winter, S. Woodward, *J. Chem. Soc. Dalton Trans.* (1988) 1449.
- [15] H.B. Friedrich, J.R. Moss, B.K. Williamson, *J. Organomet. Chem.* 394 (1990) 313.
- [16] S.F. Mapolie, Ph.D. Thesis, University of Cape Town, South Africa, 1988.
- [17] X. Yin, J.R. Moss, *J. Organomet. Chem.* 557 (1998) 259.
- [18] Y.-H. Liao, J.R. Moss, *J. Chem. Soc. Chem. Commun.* (1993) 1774.
- [19] Y.-H. Liao, J.R. Moss, *Organometallics* 14 (1995) 2130; 15 (1996) 4307.
- [20] L.G. Scott, M.Sc. Thesis, University of Cape Town, South Africa, 1984.
- [21] R.E. Dessy, R.L. Pohl, R.B. King, *J. Am. Chem. Soc.* 88 (1966) 5121.
- [22] X. Yin, Ph.D. Thesis, University of Cape Town, South Africa, 1997.
- [23] B. Giese, J. Hartung, C. Kesselheim, H.J. Lindner, I. Svoboda, *Chem. Ber.* 126 (1993) 1193.
- [24] R.B. King, M.Z. Iqbal, A.D. King Jr., *J. Organomet. Chem.* 171 (1979) 53.
- [25] C.G. Pitt, H.H. Seltzman, Y. Sayed, C.E. Twine Jr., D.L. Williams, *J. Org. Chem.* 44 (1979) 677.